Hindawi Publishing Corporation
Journal of Nanomaterials
Volume 2015, Article ID 249180, 11 pages
http://dx.doi.org/10.1155/2015/249180

Research Article

Hollow Mesoporous Silica Supported Ruthenium Nanoparticles: A Highly Active and Reusable Catalyst for H_2 Generation from the Hydrolysis of $NaBH_4$

Shuge Peng, Bingli Pan, Haijiao Hao, and Jun Zhang

Key Laboratory of Polymer and Nanomaterials, College of Chemical Engineering and Pharmacy, Henan University of Science and Technology, Luoyang 471003, China

Correspondence should be addressed to Shuge Peng; sgpeng@haust.edu.cn

Received 5 December 2014; Revised 10 February 2015; Accepted 15 February 2015

Academic Editor: Man-Rong Li

Ru nanoparticles supported on hollow mesoporous silica (HMS), which are prepared via *in situ* wet chemical reduction, have been investigated as the highly efficient heterogeneous catalyst for H_2 generation from the hydrolysis of an alkaline $NaBH_4$ solution. Many techniques, including X-ray diffraction (XRD), transmission electron microscope (TEM), and X-ray photoelectron spectroscopy (XPS), are used to characterize the as-prepared nanocatalyst (Ru/HMS). Factors, such as Ru loadings in HMS, catalyst concentration, and solution temperature, on catalytic property and reutilization are investigated in this work. A rate of H_2 generation as high as 18.6 L min^{-1} g^{-1} (Ru) using 1 wt% $NaBH_4$ solution containing 3 wt% NaOH and 40 mg of Ru/HMS catalyst can be reached at room temperature. The minimum apparent activation energy (E_a) of H_2 generation, obtained by fitting the curve of E_a values versus catalyst amount, is determined to be 46.7 ± 1 kJ/mol. The residual catalytic activity of the repeated Ru/HMS still remains 47.7% after 15 runs, which perhaps results from the incorporation of the residual by-product ($NaBO_2$) in the pores of HMS based on the analysis of XPS.

1. Introduction

Renewable energy has attracted much attention because of the ever-growing demands in energy conservation and friendly environmental protection. Moreover, an increasing number of personal electronic products also require efficient energy resources for on-board energy generation [1]. The proton-exchange membrane fuel cell (PEMFC) is thought to be the most promising fuel cell type for commercialization in future because of the high performance at low temperatures [2]. However, a safe, high-purity, and efficient H_2 production and storage have become a major concern for a PEMFC system [3]. So far, increasing attention has been paid on on-board H_2 production method, and a number of significant outcomes have been achieved [4]. Among various H_2 storage systems, chemical hydrides are widely used as candidates of hydrogen generation in terms of the portable application due to the obvious advantages, such as high H_2 capacity, well storability and controllability, low reaction-initiating temperature, and environmentally benign by-product [5].

The alkaline $NaBH_4$ solution (pH > 13) is very stable only if specific catalysts are contacted. Until now, many transition metals and alloys have been found effective in accelerating $NaBH_4$ hydrolysis [6–12]. Despite that fact that nonnoble catalysts have a cost advantage, precious metal catalysts demonstrate significantly higher catalytic activities than an equivalent amount of nonnoble catalysts [13]. To build highly efficient catalysts for $NaBH_4$ hydrolysis, the Ru-based heterogeneous catalysts still remain the preferred choice due to its price advantage among the other precious metals, such as Pt and Pd.

The activity of heterogeneous catalysts is greatly influenced by the interfaces between supporters and metal nanoparticles. To date, the most reported supports for the hydrolysis of $NaBH_4$ are mainly focused on conventional supports, like aluminum oxide (Al_2O_3), activated carbon (C), and ion-exchange resins, and so forth. Nevertheless, some ordered-structure supports, such as layered materials and mesoporous materials, have received few attention in the field

of the hydrolysis of $NaBH_4$. From our recent work, Ru nanoparticles have been successfully deposited on the external surface of montmorillonite, which greatly improved the catalytic activity due to the surface of the Ru nanoparticles (MMT) exposed. But we also found that the residual activity of the reused catalyst deteriorated, which was attributed to the aggregation and partial fall-off of the deposited Ru nanoparticles [14]. The better solution builds a more robust heterogeneous catalyst.

Because hollow mesoporous silica with available interior cavity and highly permeable mesoporous shell is convenient for the loading of different kinds of guest species, it has been widely utilized in many different fields, such as confined preparation and catalysis [15]. In view of more abundant functional groups in HMS surface than MMT, a more robust catalyst is expected to stabilize Ru nanoparticles and favor recycling nanoparticles than MMT. In our present study, hollow mesoporous silica (HMS) was used to construct Ru-based heterogeneous catalyst (Ru/HMS). And the catalytic activity and reusability of the Ru/HMS nanocatalyst were determined for H_2 evolution from the hydrolysis of an alkaline $NaBH_4$ solution. In addition, the surface morphology as well as chemistry of the reused Ru/HMS catalyst was also investigated and discussed. The effects of $NaBH_4$ and catalyst concentrations on rate of H_2 generation in low temperature were summarized in this report. Moreover, the relation of activation energy versus catalyst concentration on hydrogen production from the hydrolysis reaction was discussed in detail to optimize the catalyst amount.

2. Experimental Section

2.1. Chemicals and Materials. Ruthenium chloride hydrate ($RuCl_3 \cdot xH_2O$, Ru content ≥37%) was purchased from Sigma-Aldrich. $NaBH_4$, NaOH, and other used reagents were supplied from Sinopharm Chemical Reagent Co., Ltd. And all these chemicals are of analytical grade and used as received without further purification. Deionized water was obtained from a water purification system in our lab. Hollow mesoporous silica (HMS) was prepared according to the literature [16].

2.2. Preparation of Ru/HMS Catalyst. The Ru/HMS catalysts with different Ru laodings were prepared by *in situ* wet chemical reduction with $NaBH_4$ as the reducing agent. In a typical experiment, 2.5 g of HMS was dispersed into 200 mL of an aqueous $RuCl_3$ solution of desired concentration (1 wt%, 2 wt%, and 4 wt% of Ru with respect to HMS weight) and then mixed thoroughly by magnetic stirring at ambient temperature for 5 h to obtain Ru^{3+}/HMS, followed by the addition of an overdose of $NaBH_4$ (0.1 g) as a reducing reagent. The slurry rapidly turned into a grayish black dispersion and then was continued to stir vigorously for 1 h. Finally, catalyst powder was collected by washing using abundant deionized water to detach the other excess salt. The obtained samples were dried at 110°C for 10 h and then ground thoroughly in an agate mortar for further use.

2.3. Characterizations of Ru/HMS Catalyst. X-ray diffraction (XRD) patterns were examined using a Rigaku D/MAX-2200 diffraction using Ni-filtered Cu Kα radiation. The morphologies of the as-prepared and reused catalysts were carried out by a JEOL JSM-200CX transmission electron microscope (TEM) coupled with an energy-dispersive X-ray spectrometer (EDX). The electronic state of the surface elements was obtained from the X-ray photoelectron spectroscopy (XPS) measurement, which was performed on a VG Scientific ESCALAB 200 A spectrometer.

2.4. Evaluation of Catalytic Performance. The evaluation of the catalytic performance of the as-prepared and reused catalysts was determined by measuring the volume of H_2 evolved from the hydrolysis reaction by using a water-displacement method, which has been described in detail in our previous work [14]. During measurement, the temperature of catalytic system was monitored and carefully controlled within ±0.5°C by a thermostat.

To obtain the relationship of Ru/HMS catalyst and $NaBH_4$ concentrations on the rate of H_2 evolution from the hydrolysis of alkaline $NaBH_4$ catalyzed by the as-prepared Ru/HMS catalyst, the $NaBH_4$ hydrolysis was firstly performed with different catalyst amounts (10, 20, 40, and 80 mg) while keeping $NaBH_4$ (1 wt%) and NaOH concentration (3 wt%) constant; and then varying the concentration of $NaBH_4$ (1, 2.5, 5, and 10 wt%) when catalyst amount (10 mg) and NaOH concentration (3 wt%) are kept constant. To obtain the minimum E_a value, the relationship of E_a value versus catalyst amount is determined. The different catalyst amounts, that is, 10, 20, 40, and 80 mg, are used to catalyze $NaBH_4$ hydrolysis under constant $NaBH_4$ (1 wt%) and NaOH (3 wt%) under different temperatures ranged from 10°C to 30°C, respectively.

3. Results and Discussion

3.1. Characterization of Ru/HMS Catalyst. The aim of this investigation is to develop a facile and efficient method for preparing Ru/HMS nanocomposites as catalyst for the H_2 production from an alkaline $NaBH_4$ solution. Figure 1 shows the XRD patterns of the pristine HMS and Ru/HMS samples with different loadings in the small-angle range. As indicated in Figure 1(a), the pattern gives three well-resolved Bragg diffraction peaks, which can be attributed to the (100), (110), and (200) reflections of a hexagonal symmetry structure typical for MCM-41. The result is in accordance with those of the reported data [16], indicating the successful preparation of HMS. After being loaded with Ru nanoparticles, the Bragg diffraction intensities of these samples (Ru/HMS) become weaker compared with those of the pristine HMS; and with the Ru loading increasing, the intensity of the Bragg diffraction decreases. XRD results indicate that Ru nanoparticles have been successfully loaded in HMS, and the mesoporous structure of HMS is still remaining after being loaded with Ru nanoparticles.

The existence of Ru nanoclusters in HMS is further investigated by TEM measurements. Figure 2(a) shows a typical TEM image of the as-prepared Ru/HMS nanocomposites. As observed in the figure, sphere morphology with the size of

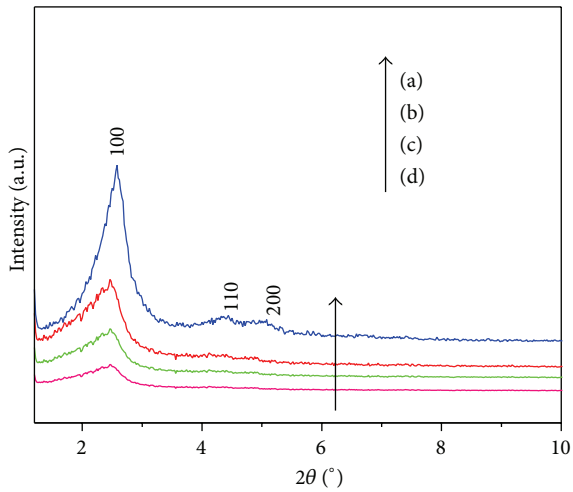

Figure 1: X-ray diffraction patterns of the host material HMS and the HMS confined Ru(0) (Ru/HMS) with different loadings. (a) HMS; (b) 1 wt% of Ru loading; (c) 2 wt% of Ru loading; (d) 4 wt% of Ru loading.

2-3 μm or so is clearly observed. And there is an obvious contrast between the core and the shell of the Ru/HMS sphere in the micrograph. The result of TEM image further proved that the synthesized HMS sphere has a hollow structure, which is in accordance with the reference. Further observed from the TEM micrograph with greater enlargement of Ru/HMS sample (Figure 2(b)), the thickness of the shells can be estimated in the range of 100–200 nm. The TEM image of the loaded Ru particles in the hollow region (Figure 2(c)) demonstrates many dark nanoparticles, and these particles should be assigned to be Ru nanoparticles, which is proved by the EDX result (Figure 2(f)). As indicated in the figure, the elemental Ru clearly exists in the catalyst sample. Furthermore, broad rings are shown in the electron diffraction (ED) pattern of the as-prepared Ru/HMS sample (Figure 2(e)), implying the nanocrystalline phase is formed. According to the diffraction rings, the *d-spacings* could be calculated to be 1.93 and 1.21 Å, which corresponds to the reflections of the (101) and (103) lattice planes of hexagonal close packed metal Ru, respectively [17]. As observed from the size distribution of the loaded Ru nanoparticles in Figure 2(d), the deposited particle size ranged from 10 nm to 42 nm, with a mean value of 23.4 nm. TEM results further prove that Ru nanoparticles have been successfully loaded in HMS, which is accordance with the result of XRD.

XPS measurements are used to further determine whether metallic Ru(0) nanostructures have been formed in Ru/HMS samples. The results are shown in Figure 3. From the survey spectrum (Figure 3(a)), the binding energies at 489.1 and 468.1 eV can be assigned to the characteristic peaks of Ru $3p_{1/2}$ and Ru $3p_{3/2}$, respectively; and the peak at 289.1 eV is ascribed to the characteristic peak of Ru 3*d* [18], further conforming the formation of metallic Ru(0) by *in situ* wet chemical reduction. Additionally, there exists Ru-O component in the high-resolution XPS at the Ru *3d* except Ru^0 in Ru/HMS catalyst (Figure 3(b)), which is probably due to the partial oxidation of the loaded Ru nanoclusters upon exposure to air at ambient temperature. Based on the XPS quantitative analysis, the experimental amount of Ru loaded in the HMS is calculated as 2.3 wt%, which is close to 2 wt%, the theoretical amount of Ru in HMS.

3.2. Evaluation of Catalytic Activity

3.2.1. Effect of Ru Loading. The plot of time-dependent H_2 generation from an alkaline $NaBH_4$ solution catalyzed by Ru/HMS with different loadings is shown in Figure 4. With HMS, nearly no H_2 generation produced. However, in the presence of Ru/HMS catalyst, the hydrolysis reaction immediately starts upon contact of the catalyst with the $NaBH_4$ solution. In addition, the linear increase in H_2 generation enables a continuable and controllable H_2 generation process for practical applications. Upon reaching a certain time, H_2 generation stops. The total H_2 yield reached 99% of the theoretically expected value. The catalytic performance is expected to depend on Ru loadings of Ru/HMS sample. Accordingly, the catalytic activity of Ru/HMS samples (in all the same amount of catalyst) with different Ru loadings in Ru/HMS was tested in the hydrolysis of alkaline $NaBH_4$ solution to determine the effect of Ru loading on the catalytic activity. As indicated in Figure 4(b), the rate of H_2 generation is the greatest when the Ru loading in Ru/HMS is 2.3 wt%. As the Ru loading increases, perhaps some of the Ru nanoclusters become larger, blocking the entrance to the interior cavity [19].

As displayed in Figure 4(a), H_2 can be totally released within 1200 s in the hydrolysis system with 40 mg of Ru/HMS loaded with 2.3 wt% Ru ($Ru/NaBH_4$ molar ratio = 0.003), and an average rate of H_2 generation reaches 18600 ± 500 mL · min^{-1} · $g(Ru)^{-1}$ at 25°C. The H_2 generation rate of Ru/HMS catalyst is lower than our previously reported value of Ru/MMT, which might be due to the confinement of the mesoporous shell of HMS. But the catalytic activity of Ru/HMS is still higher than those of most Ru-based heterogeneous catalysts used in the same catalytic system, like Ru/IRA-120, Ru/carbon, Ru/zeolite-Y, and so forth indicating that Ru/HMS is a high-efficiency catalyst for $NaBH_4$ hydrolysis. Accordingly, the sample with a 2.3 wt% Ru loading is used in the followed experiments for the further investigation.

3.2.2. Rate Equation of $NaBH_4$ Hydrolysis. To identify the reaction order with catalyst amount, the H_2 evolution rate is measured by using different catalyst amounts (10, 20, 40, and 80 mg) in the presence of 1 wt% $NaBH_4$ and 3 wt% NaOH. As shown in Figure 5(a), the addition of even a small amount of Ru/HMS rapidly triggered the hydrolysis of alkaline $NaBH_4$ with no obvious induction period. And the more the catalyst amount is, the shorter the reaction time required for completing the hydrolysis reaction is. For minimizing the measurement error, the initial stage of $NaBH_4$ hydrolysis was analyzed to determine the H_2 generation rate, which was then correlated with the catalyst amount to quantitatively estimate its effect on the above-mentioned rate. The H_2 generation rate (mL s^{-1}) was then plotted against

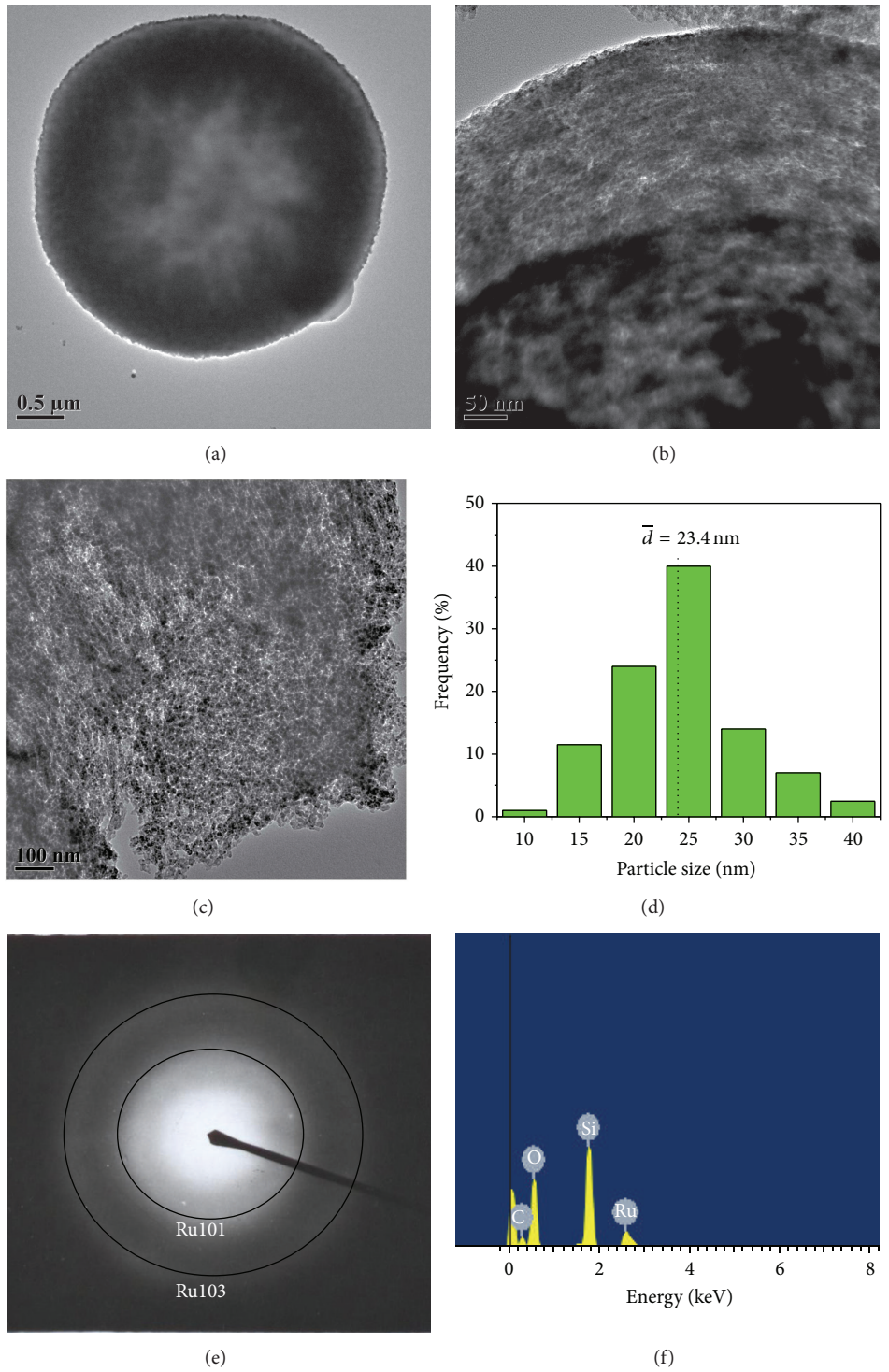

FIGURE 2: TEM images of Ru/HMS with different magnification times ((a) and (b)), TEM image (c), size distribution (d), and SAED pattern (e) of the deposited Ru nanoparticles and EDS results (f) of Ru/HMS with a Ru loading of 2.3 wt%.

the Ru/HMS catalyst amount (mg), with both terms in the logarithmic scale (Figure 5(b)). A best-fit straight line with the correlation coefficient, $R^2 = 0.989$, is obtained. The slope is $1.12 \approx 1$, demonstrating that the hydrolysis reaction is quasi-first-order with respect to the supplied amount of Ru/HMS. A similar result was also reported by Özkar group in the study of the ammonia borane hydrolysis catalyzed by nanotitania supported Ru nanoparticles [20].

The effect of $NaBH_4$ loading (1, 2.5, 5, and 10 wt%) in the presence of 3 wt% NaOH and 10 mg Ru/HMS catalyst on

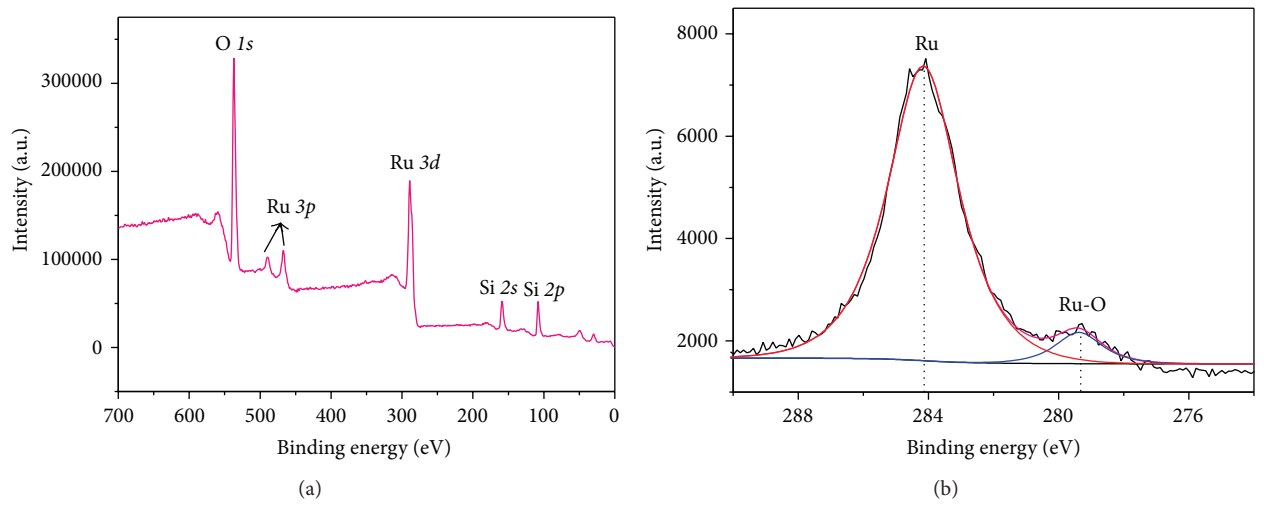

(a) (b)

FIGURE 3: Plots of survey XPS (a) and high-resolution XPS at the Ru *3d* (b) for the as-prepared Ru/HMS catalyst. The two vertical lines indicate the peak positions of Ru and Ru-O, respectively.

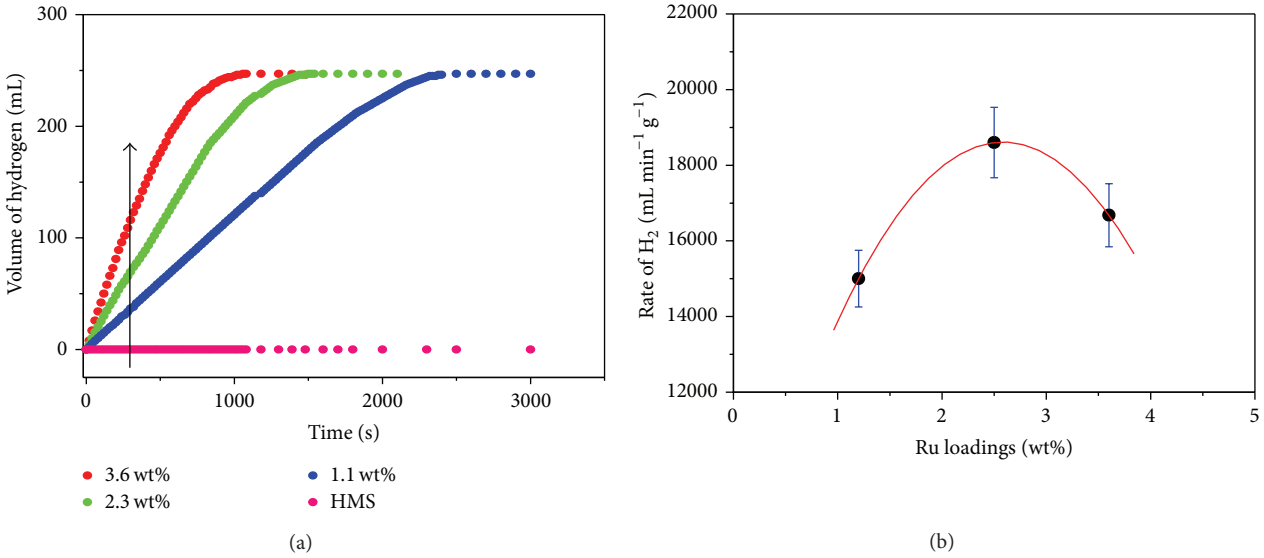

(a) (b)

FIGURE 4: (a) Volume of H_2 generated as a function of time from 1 wt% $NaBH_4$ + 3 wt% NaOH solutions at 25°C using 40 mg of Ru/HMS with different Ru loadings and HMS. (b) The plot of H_2 generation rate versus Ru loading.

the H_2 generation rate at 25°C is shown in Figure 6(a). As the $NaBH_4$ concentrations increase from 1 wt% to 10 wt%, the H_2 generation rate slightly increased. Generally speaking, an increase in the substrate concentration can generally lead to an increase in the product generation rate. As substrate concentration increases, the solution viscosity also increases. Moreover, the aqueous solubility of $NaBO_2$ (by-product) is low. Accordingly, all these effects in turn lead to the decrease in the H_2 generation rate [21]. The effect of $NaBH_4$ loading on the H_2 generation rate was also determined by analyzing the initial stage of $NaBH_4$ hydrolysis. From Figure 6(b), a well-fitted straight line with the correlation coefficient, $R^2 = 0.97$, is yielded. The slope is $0.16 \approx 0$, indicating that the hydrolysis of $NaBH_4$ is zero-order with respect to the supplied $NaBH_4$ loading. Yu group and Özkar group also reported similar phenomenon [22, 23].

Based on the above analysis, the rate law of the $NaBH_4$ hydrolysis catalyzed by Ru/HMS can be presented, as shown in

$$\frac{-4d\left[\mathrm{NaBH_4}\right]}{dt} = \frac{d\left[\mathrm{H_2}\right]}{dt} = k\left[\mathrm{Ru}\right], \quad (1)$$

where k is the rate constant. In view of the effect of $NaBH_4$ loading on the hydrolysis of $NaBH_4$, the zero-order kinetics of $NaBH_4$ loading is limited to below 10 wt% in our study.

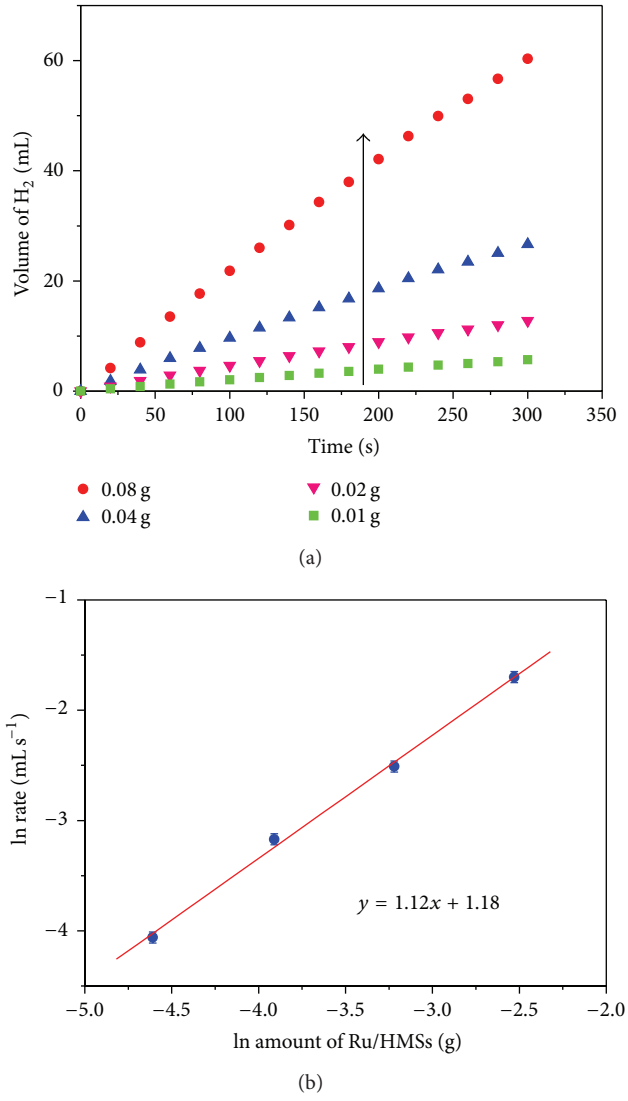

Figure 5: (a) Volume of H_2 generation against Ru/HMS amount from 1 wt% $NaBH_4$ and 3 wt% NaOH at 25°C. (b) The plot of H_2 generation rate versus Ru/HMS amount.

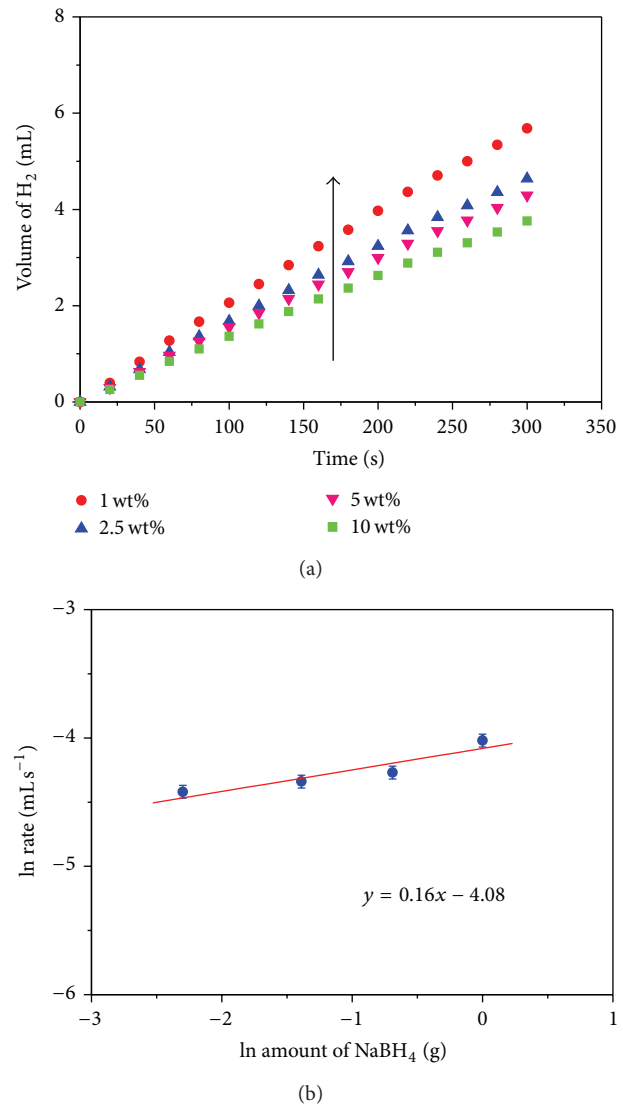

Figure 6: (a) Volume of H_2 generation versus $NaBH_4$ concentration from x wt% $NaBH_4$ + 3 wt% NaOH + 0.01 g Ru/HMS catalyst at 25°C. (b) The plot of H_2 generation rate versus the $NaBH_4$ amount.

3.2.3. Activation Energy of $NaBH_4$ Hydrolysis. Hydrolysis kinetics is thought to be a complex process, which is influenced by many factors, like catalyst performance, temperature, $NaBH_4$ concentration, and so forth. Among them, water is an important reactant for $NaBH_4$ hydrolysis and also solvent for the reactants and by-products [24]. An optimal catalyst amount is expected when the others remain unchanged in $NaBH_4$ hydrolysis reaction. The optimal catalyst amount is evaluated by the value of activation energy (E_a). Accordingly, the $NaBH_4$ hydrolysis kinetics is further investigated at different catalyst amount. The effects of temperatures (ranged from 10°C to 30°C) on the rate of H_2 evolved in solutions containing 1 wt% $NaBH_4$ + 3 wt% NaOH and different Ru/HMS amount, that is, 10 mg, 20 mg, 40 mg, and 80 mg, respectively, are shown in Figure 7. As expected, the rate of H_2 generation increases with the temperature. According to Arrhenius equation, the rate constant can be expressed in logarithmic function form, as shown in

$$\ln k = -\frac{E_a}{R\,(1/T)} + \ln k_0, \tag{2}$$

where k is the rate constant, k_0 is the preexponential parameter, E_a is the activation energy, R is the gas constant (8.314 J · mol^{-1} · K^{-1}), and T is the reaction temperature. According to (1), the rate constant k under different catalyst amount can be calculated from the data shown in Figures 7(A)~7(D), respectively. Then the corresponding Arrhenius plots, ln k versus the reciprocal absolute temperature ($1/T$), are shown in Figures 7(a)~7(d), respectively. The slopes of these fitted straight lines were −11.1, −9.8, −6.02, and −7.69, corresponding to 10 mg, 20 mg, 40 mg, and 80 mg of Ru/HMS catalyst, respectively. According to the Arrhenius relationship

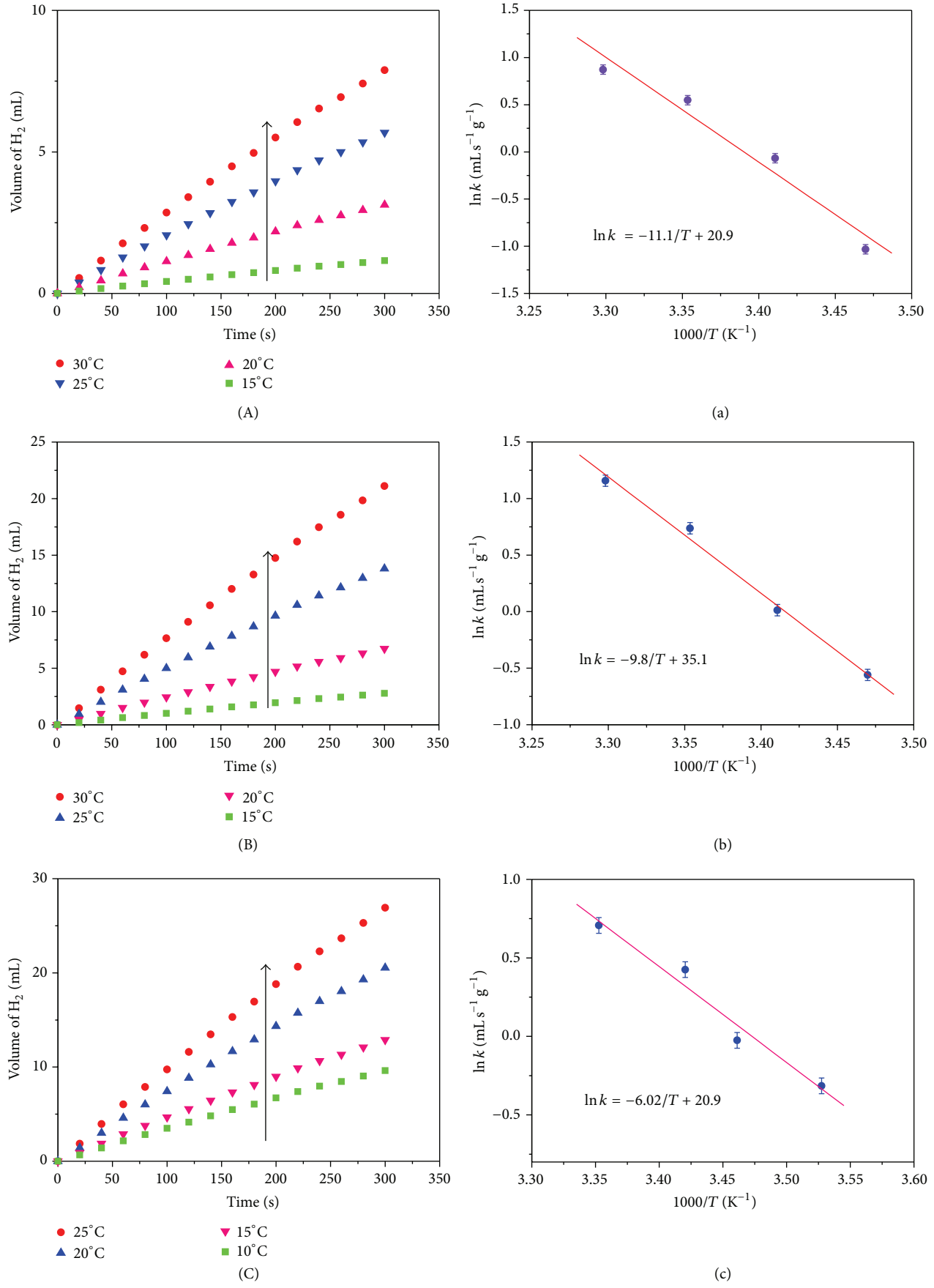

Figure 7: Continued.

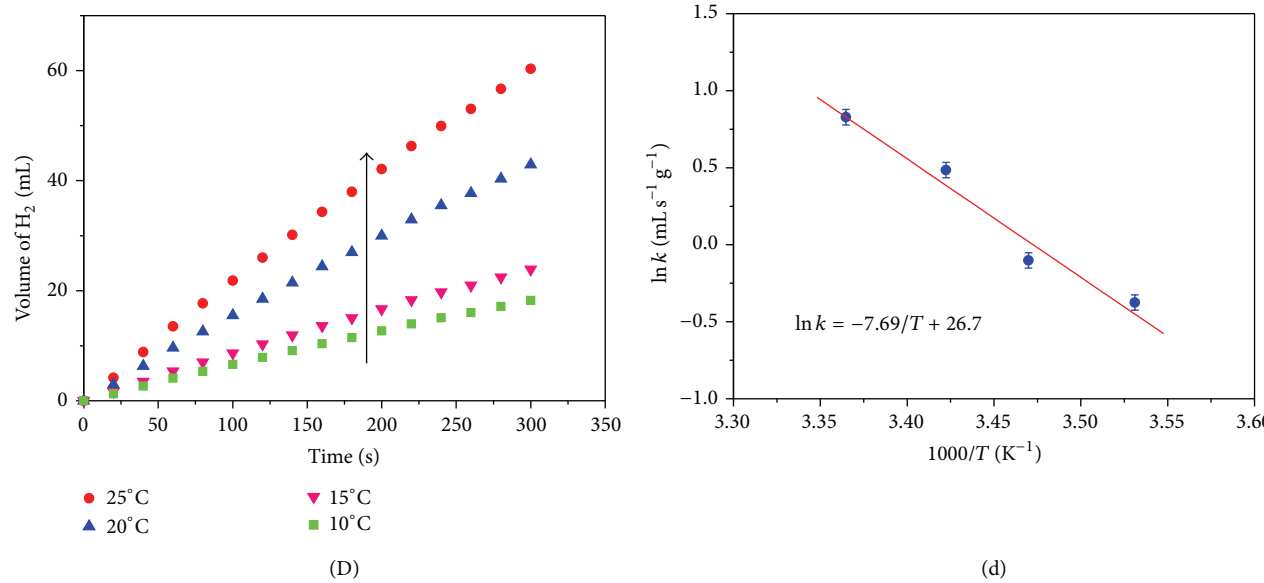

FIGURE 7: Volume of H_2 generation against temperature from 1 wt% $NaBH_4$ + 3 wt% NaOH + x g Ru/HMS catalyst and the ln k versus $1/T$ plots. The error bars reflect around ±5% measurement error of the H_2 generation rate. ((A) and (a)) 0.01 g Ru/HMS; ((B) and (b)) 0.02 g Ru/HMS; ((C) and (c)) 0.04 g Ru/HMS; ((D) and (d)) 0.08 g Ru/HMS.

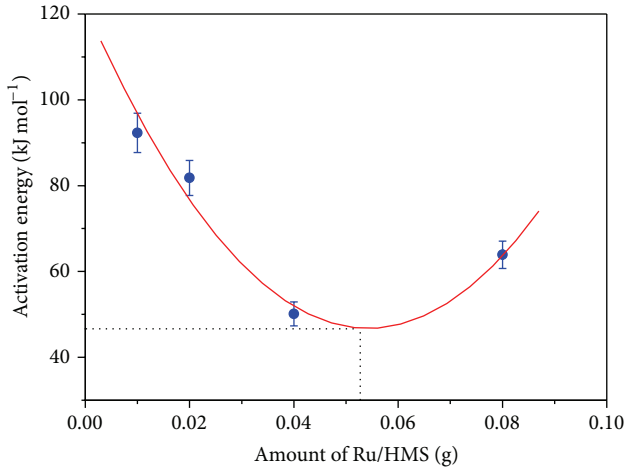

FIGURE 8: Activation energy as a function of Ru/HMS amount for the $NaBH_4$ hydrolysis.

"(2)," the apparent E_a values for the Ru/HMS-catalyzed hydrolysis of $NaBH_4$ are calculated as 93.3 ± 1, 81.8 ± 1, 50.1 ± 1, and 63.9 ± 1 kJ/mol, respectively. The dependence of apparent E_a value on the catalyst amount is also found in our recent work of Ru/MMT-catalyzed $NaBH_4$ hydrolysis [25].

To observe clearly the changes of apparent E_a value with catalyst amount, Figure 8 shows the dependence of E_a value on the catalyst amount when the other catalytic conditions keep the same. It is clearly seen that there exists a valley value between the E_a value and catalyst amount. Accordingly, the minimum apparent E_a value can be deduced to be 46.2 ± 1 kJ/mol when the Ru/HMS amount is 52.5 mg. It is commonly believed that the availability of catalytically active sites increases with catalyst amount increasing, and accordingly, lower apparent E_a value should be obtained. However, increased apparent E_a value is observed when an excessive catalyst amount is used. The possible reason is that the excess Ru/HMS amount would absorb much water into its pore and hollow region, which resulted in an increased solution viscosity of catalytic system. Accordingly, it becomes difficult for the $NaBH_4$ molecules to further contact these catalytic active sites and give rise to the mass transport limitations. On the other hand, the low aqueous solubility of by-product, $NaBO_2$, would also produce precipitation of $NaBO_2{\cdot}4H_2O$, and two effects might exist: one is to interfere in the mass transfer between Ru/HMS and $NaBH_4$; the other is to wrap the surface of Ru/HMS to cover up active sites of catalysts and further prevent $NaBH_4$ from hydrolysis over active sites [26]. Apparently, there exists an optimal catalyst amount during $NaBH_4$ hydrolysis. It is important to determine the optimal catalyst amount for optimizing the operating conditions to minimize the use of water in the hydrolysis of $NaBH_4$.

Numerous investigations have shown that the studies on the kinetics of the heterogeneous reaction of metal-catalyzed $NaBH_4$ hydrolysis face two challenges, that is, the controls of temperature and pH during the reaction and the reaction kinetics changes with catalytic conditions, such as catalyst amount, substrate concentration, solution temperature, and reaction time [27]. In our tests, the kinetics of Ru/HMS-catalyzed $NaBH_4$ hydrolysis is measured under lower temperatures and higher alkalinity to overcome the negative effects by temperature and pH value. Compared to the reported apparent E_a values obtained in the $NaBH_4$ hydrolysis as catalyzed by other Ru-based catalysts [14], the apparent E_a value of the as-prepared Ru/HMS is lower than most of previously reported values except 37.3 kJ/mol for Ru/carbon [28] and 34.9 kJ/mol for Ru/zeolite [29].

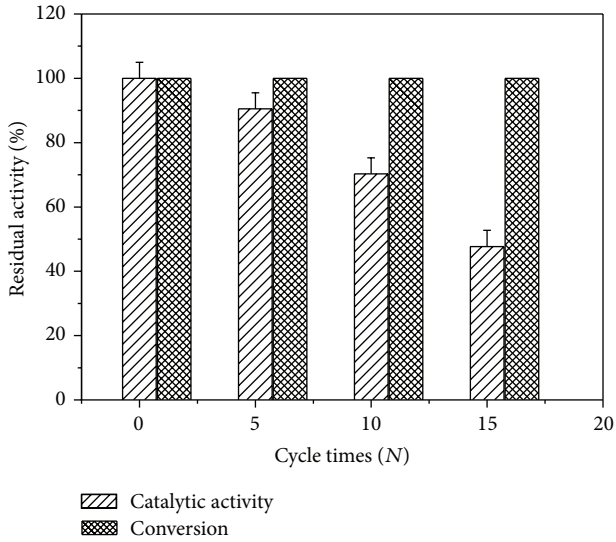

FIGURE 9: Remaining catalytic activity and the conversion of $NaBH_4$ versus cyclic runs of the Ru/HMS from 1 wt% $NaBH_4$ + 3 wt% NaOH + 0.04 g of Ru/HMS catalyst at 25°C.

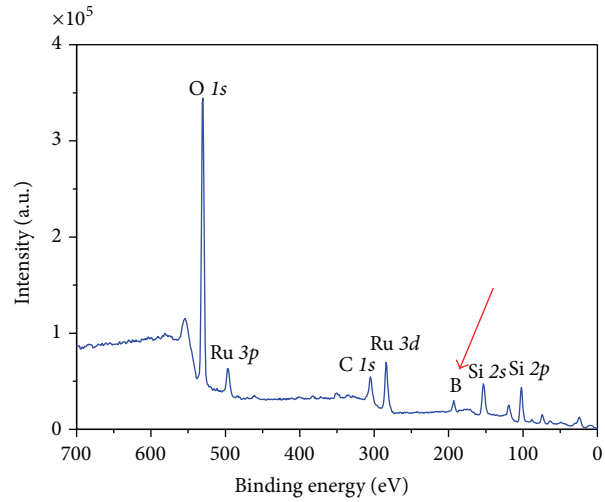

FIGURE 10: The plot of survey XPS spectrum of the reused Ru/HMS catalyst.

3.3. Reusability of Ru/HMS Catalyst. Catalyst reusability is significant in practical application for the H_2 generation. In our study, the reusability of the Ru/HMS was measured by repeating $NaBH_4$ hydrolysis experiment fifteen times catalyzed by the recycled Ru/HMS batch. After each run, the catalyst was separated from the catalytic mixture by centrifugation and thoroughly washed with copious water to remove the soluble salts. The remaining activity against the cycle time from 1 wt% $NaBH_4$ + 3 wt% NaOH solution and 40 mg Ru/HMS at 25°C is shown in Figure 9. As indicated in Figure 9, the remaining activity of Ru/HMS catalyst in the fifth run is only slightly inferior to the initial catalytic activity. The catalyst still preserves 47.7% of its initial catalytic activity and maintains a complete release of H_2 at the 15th runs. The reusability indicates that the Ru/HMS catalyst is separable, redispersible, and yet catalytically active.

To explain the decreased activity of the reused Ru/HMS-catalyzed $NaBH_4$ hydrolysis in an alkaline solution, XPS is used to detect the chemical changes of the reused Ru/HMS after 15 runs to investigate the reason of the catalytic deterioration of the reused Ru/HMS. As shown in Figure 10, there exists a new peak around 193 eV, which is ascribed to $NaBO_2$ or B_2O_3. The new peak shifts to higher binding energy than elemental B, which is probably due to oxidation. Accordingly, the decreased catalytic activity in subsequent cycles might result from the incorporation of the by-product ($NaBO_2$) in the pores of HMS, which would passivate the surface of Ru nanoclusters and decrease the access to active sites. Dai et al. in their study of the Ru/MMT-catalyzed hydrolysis of ammonia borane also reported similar result [30]. Additionally, the decreased activity also might result from the catalyst material loss during the separation and redispersion [31].

4. Conclusions

In summary, a facile method for preparing the Ru/HMS composites as highly active nanocatalyst is developed for hydrolyzing sodium borohydride from its alkaline solution. Different Ru loadings in Ru/HMS are successfully achieved, and the Ru/HMS with a Ru loading of 2.3 wt% shows the highest catalytic activity. When the Ru/HMS catalyst with a Ru loading of 2.3 wt% is used, a maximum H_2 generation rate of 18.6 L min^{-1} g^{-1}(Ru) from 1 wt% $NaBH_4$ + 3 wt% NaOH solutions at 25°C is obtained. The relation of activation energy versus catalyst amount is constructed to optimize the catalyst amount; and the minimum apparent E_a value obtained from the fitted curve is 46.2 ± 1 kJ/mol when the catalyst amount was 52.5 mg, lower than the E_a values of most Ru-based heterogeneous catalysts reported in literatures. Moreover, the reusability of the catalyst shows that the remaining activity of Ru/HMS catalyst in the fifth run is only slightly inferior to that in the first run, when, at the fifteen times of usage, the catalyst still preserves 47.7% of its initial catalytic activity. The decreased catalytic activity in subsequent cycles might result from the incorporation of the by-product ($NaBO_2$) in the pores of HMS, which would passivate the surface of Ru nanoclusters and decrease the access to active sites.

Conflict of Interests

The authors declare that there is no conflict of interests regarding the publication of this paper.

Acknowledgment

This work was financially supported by the Natural Science Foundation of China under Contract nos. 21101058 and 51105130.

References

[1] B. H. Liu and Z. P. Li, "A review: hydrogen generation from borohydride hydrolysis reaction," *Journal of Power Sources*, vol. 187, no. 2, pp. 527–534, 2009.

[2] D. M. F. Santos and C. A. C. Sequeira, "Sodium borohydride as a fuel for the future," *Renewable and Sustainable Energy Reviews*, vol. 15, no. 8, pp. 3980–4001, 2011.

[3] Z.-H. Lu and Q. Xu, "Recent progress in boron- and nitrogen-based chemical hydrogen storage," *Functional Materials Letters*, vol. 5, Article ID 12300010, 9 pages, 2012.

[4] L. Schlapbach and A. Züttel, "Hydrogen-storage materials for mobile applications," *Nature*, vol. 414, no. 6861, pp. 353–358, 2001.

[5] U. Eberle, M. Felderhoff, and F. Schüth, "Chemical and physical solutions for hydrogen storage," *Angewandte Chemie International Edition*, vol. 48, no. 36, pp. 6608–6630, 2009.

[6] J. Yang, A. Sudik, C. Wolverton, and D. J. Siegel, "High capacity hydrogen storage materials: attributes for automotive applications and techniques for materials discovery," *Chemical Society Reviews*, vol. 39, no. 2, pp. 656–675, 2010.

[7] M. Rakap and S. Özkar, "Intrazeolite cobalt(0) nanoclusters as low-cost and reusable catalyst for hydrogen generation from the hydrolysis of sodium borohydride," *Applied Catalysis B: Environmental*, vol. 91, no. 1-2, pp. 21–29, 2009.

[8] Z.-H. Lu, Q. Yao, Z. Zhang, Y. Yang, and X. Chen, "Nanocatalysts for hydrogen generation from ammonia borane and hydrazine borane," *Journal of Nanomaterials*, vol. 2014, Article ID 729029, 11 pages, 2014.

[9] Z.-H. Lu, Q. L. Yao, Z. J. Zhang, Y. W. Yang, and X. S. Chen, "Nanocatalysts for hydrogen generation from ammonia borane and hydrazine borane," *Journal of Nanomaterials*, vol. 2014, Article ID 729029, 11 pages, 2014.

[10] Y. Yang, F. Zhang, H. Wang, Q. Yao, X. Chen, and Z.-H. Lu, "Catalytic hydrolysis of ammonia borane by cobalt nickel nanoparticles supported on reduced graphene oxide for hydrogen generation," *Journal of Nanomaterials*, vol. 2014, Article ID 294350, 9 pages, 2014.

[11] N. Patel, R. Fernandes, and A. Miotello, "Promoting effect of transition metal-doped Co-B alloy catalysts for hydrogen production by hydrolysis of alkaline $NaBH_4$ solution," *Journal of Catalysis*, vol. 271, no. 2, pp. 315–324, 2010.

[12] M. Kurtinaitiene, A. Žieliene, L. Tamašauskaite-Tamašiunaite, A. Selskis, and A. Jagminas, "Hydrothermal synthesis of Co-Ru alloy particle catalysts for hydrogen generation from sodium borohydride," *Advances in Materials Science and Engineering*, vol. 2013, Article ID 489840, 7 pages, 2013.

[13] H. C. Brown and C. A. Brown, "New, highly active mental catalysts for the hydrolysis of borohydride," *Journal of the American Chemical Society*, vol. 84, no. 8, pp. 1493–1494, 1962.

[14] S. Peng, X. Fan, J. Zhang, and F. Wang, "A highly efficient heterogeneous catalyst of Ru/MMT: preparation, characterization, and evaluation of catalytic effect," *Applied Catalysis B: Environmental*, vol. 140-141, pp. 115–124, 2013.

[15] X. Fang, X. Zhao, W. Fang, C. Chen, and N. Zheng, "Self-templating synthesis of hollow mesoporous silica and their applications in catalysis and drug delivery," *Nanoscale*, vol. 5, no. 6, pp. 2205–2218, 2013.

[16] Y. Zhu, J. Shi, H. Chen, W. Shen, and X. Dong, "A facile method to synthesize novel hollow mesoporous silica spheres and advanced storage property," *Microporous and Mesoporous Materials*, vol. 84, no. 1–3, pp. 218–222, 2005.

[17] P. Krishnan, T.-H. Yang, W.-Y. Lee, and C.-S. Kim, "PtRu-$LiCoO_2$—an efficient catalyst for hydrogen generation from sodium borohydride solutions," *Journal of Power Sources*, vol. 143, no. 1-2, pp. 17–23, 2005.

[18] S. Peng, C. Liu, X. Liu, J. Zhang, and Y. Zhang, "Water dispersible Ru (0) nanorods: a highly efficient heterogeneous catalyst for the hydrogen generation from sodium borohydride solutions," *Integrated Ferroelectrics*, vol. 135, no. 1, pp. 47–54, 2012.

[19] M. Zahmakiran, T. Kodaira, and S. Özkar, "Ruthenium(0) nanoclusters stabilized by zeolite framework as superb catalyst for the hydrogenation of neat benzene under mild conditions: Additional studies including cation site occupancy, catalytic activity, lifetime, reusability and poisoning," *Applied Catalysis B: Environmental*, vol. 96, no. 3-4, pp. 533–540, 2010.

[20] S. Akbayrak, S. Tanyildizi, I. Morkan, and S. Özkar, "Ruthenium(0) nanoparticles supported on nanotitania as highly active and reusable catalyst in hydrogen generation from the hydrolysis of ammonia borane," *International Journal of Hydrogen Energy*, vol. 39, no. 18, pp. 9628–9637, 2014.

[21] S. S. Muir and X. Yao, "Progress in sodium borohydride as a hydrogen storage material: development of hydrolysis catalysts and reaction systems," *International Journal of Hydrogen Energy*, vol. 36, no. 10, pp. 5983–5997, 2011.

[22] A.-J. Hung, S.-F. Tsai, Y.-Y. Hsu, J.-R. Ku, Y.-H. Chen, and C.-C. Yu, "Kinetics of sodium borohydride hydrolysis reaction for hydrogen generation," *International Journal of Hydrogen Energy*, vol. 33, no. 21, pp. 6205–6215, 2008.

[23] Ö. Metin and S. Özkar, "Synthesis and characterization of poly(N-vinyl-2-pyrrolidone)-stabilized water-soluble nickel(0) nanoclusters as catalyst for hydrogen generation from the hydrolysis of sodium borohydride," *Journal of Molecular Catalysis A: Chemical*, vol. 295, no. 1-2, pp. 39–46, 2008.

[24] R. Retnamma, A. Q. Novais, and C. M. Rangel, "Kinetics of hydrolysis of sodium borohydride for hydrogen production in fuel cell applications: a review," *International Journal of Hydrogen Energy*, vol. 36, no. 16, pp. 9772–9790, 2011.

[25] S. Peng, X. Fan, Y. Wu, and J. Zhang, "Kinetic study of hydrogen generation from the hydrolysis of alkaline $NaBH_4$ over Ru/MMT: an insight on the effect of catalyst amount," *Integrated Ferroelectrics*, vol. 147, no. 1, pp. 159–165, 2013.

[26] Y. Liang, H.-B. Dai, L.-P. Ma, P. Wang, and H.-M. Cheng, "Hydrogen generation from sodium borohydride solution using a ruthenium supported on graphite catalyst," *International Journal of Hydrogen Energy*, vol. 35, no. 7, pp. 3023–3028, 2010.

[27] Y. Shang, R. Chen, and G. Jiang, "Kinetic study of $NaBH_4$ hydrolysis over carbon-supported ruthenium," *International Journal of Hydrogen Energy*, vol. 33, no. 22, pp. 6719–6726, 2008.

[28] Y. Shang and R. Chen, "Semiempirical hydrogen generation model using concentrated sodium borohydride solution," *Energy and Fuels*, vol. 20, no. 5, pp. 2149–2154, 2006.

[29] M. Zahmakiran and S. Özkar, "Zeolite-confined ruthenium(0) nanoclusters catalyst: record catalytic activity, reusability, and lifetime in hydrogen generation from the hydrolysis of sodium borohydride," *Langmuir*, vol. 25, no. 5, pp. 2667–2678, 2009.

[30] H.-B. Dai, X.-D. Kang, and P. Wang, "Ruthenium nanoparticles immobilized in montmorillonite used as catalyst for methanolysis of ammonia borane," *International Journal of Hydrogen Energy*, vol. 35, no. 19, pp. 10317–10323, 2010.

[31] M. Rakap and S. Özkar, "Zeolite confined palladium(0) nanoclusters as effective and reusable catalyst for hydrogen generation from the hydrolysis of ammonia-borane," *International Journal of Hydrogen Energy*, vol. 35, no. 3, pp. 1305–1312, 2010.